Radiology

Hyperpolarized ^{129}Xe MRI Abnormalities in Dyspneic Participants 3 Months after COVID-19 Pneumonia: Preliminary Results

Manuscript Type: Original Research

James T. Grist, PhD, BSc[1,2,3,4], Mitchell Chen, BMBCh, MEng, DPhil, FRCR[3], Guilhem J. Collier[5], PhD, Betty Raman, MBBS, DPhil[2], Gabriele AbuEid, BSc[3], Anthony McIntyre, BAppSc[3], Violet Matthews, BSc[3], Emily Fraser, PhD, MBChB, BSc[7], Ling-Pei Ho, MD, PhD[6,7], Jim M. Wild, PhD, MSc, MA[5], Fergus Gleeson, MBBS[3,8]

1 Department of Physiology, Anatomy, and Genetics, University of Oxford, Oxford
2 Oxford Centre for Clinical Magnetic Resonance Research, University of Oxford, Oxford
3 Department of Radiology, The Churchill Hospital, Oxford NHS Foundation Trust, Oxford
4 Institute of Cancer and Genomic Sciences, University of Birmingham, Birmingham
5 POLARIS, Department of Infection Immunity and Cardiovascular Disease, University of Sheffield
6 MRC Human Immunology Unit, University of Oxford
7 Oxford Interstitial Lung Disease Service, Oxford NHS Foundation Trust
8 Department of Oncology, University of Oxford, Oxford

Corresponding author details: Professor Fergus Gleeson, Department of Oncology, University of Oxford, Old Road, Headington, Oxford 0X3 7DQ, England
e-mail: fergus.gleeson@oncology.ox.ac.uk

Funding: Dr Grist is funded by the Biomedical Research Centre, Oxford. LPH is supported in part by the NIHR Biomedical Research Centre, Oxford. Collier and Wild are funded by MRC grant MR/M008894/1. Dr Betty Raman is funded by the British Heart Foundation Oxford Centre for Research Excellence (RE/18/3/34214).
This work was supported by the National Consortium of Intelligent Medical Imaging through the Industry Strategy Challenge Fund, Innovate UK Grant 104688.

See also the editorial by Dietrich.

Summary

For dyspneic patients 3 months after discharge from the hospital for COVID-19, hyperpolarized ^{129}Xe MRI showed abnormalities due to gas transfer limitation in the lungs.

Key Results

- In nine patients evaluated at 3 months post hospital discharge for COVID-19, hyperpolarized ^{129}Xe MRI identifies regional RBC:TP abnormalities, in comparison to healthy controls, (0.3 ± 0.1 versus 0.5 ± 0.1, respectively, p = 0.001, effect size = 1.36) despite structurally normal/near normal lungs on CT post COVID-19 pneumonia.
- Hyperpolarized ^{129}Xe MRI gas transfer abnormalities are present post COVID-19 pneumonia even when patient clinical measurements such as D-dimer, hemoglobin and lung function tests are within normal range.
- These abnormalities were detected in the presence of contemporaneous normal/near normal CT scans (mean score = 7/25, range = 0-10/25).

Abstract

Background: SARS-CoV-2 targets angiotensin-converting enzyme 2 (ACE2) expressing cells in the respiratory tract. There are reports of breathlessness in patients many months post-infection.

Purpose: This study aimed to determine if hyperpolarized ^{129}Xe MRI (XeMRI) imaging could identify the possible cause of breathlessness in patients three months after hospital discharge following COVID-19 infection.

Materials and Methods: This prospective study was undertaken between August and December 2020, with patients and healthy control volunteers enrolled. All patients underwent: lung function tests; ventilation and dissolved phase XeMRI, with the mean Red Blood Cell (RBC):Tissue Plasma (TP) ratio to be calculated; and a low dose chest CT scored for the degree of post-COVID-19 abnormalities. Healthy controls underwent XeMRI. The intraclass correlation coefficient was calculated for volunteer and patient scans, to assess repeatability. A Wilcoxon rank-sum test and Cohen's effect size calculated to assess for differences between RBC:TP in patient and controls.

Results: 9 patients (mean age 57±7 years, Male = 6) and 5 volunteers (29 ± 3 years, Female = 5) were enrolled. Patient mean time from hospital discharge was 169, range 116-254 days. There was a difference in RBC:TP between patients and controls (0.3 ± 0.1 versus 0.5 ± 0.1, respectively, p = 0.001, effect size = 1.36). There was significant difference between the RBC and gas phase spectral full width at half maximum (FWHM) between volunteers and patients (median ± 95 % confidence interval, 567 ± 1 vs 507 ± 81, p = 0.002 and 104 ± 2 vs 122 ± 17, p = 0.004, respectively). Results were reproducible with Intraclass Correlation Coefficients of 0.82 and 0.88 for patients and volunteers respectively. Participants had normal or near normal CT scans, mean 7/25, range 0-10/25.

Conclusion: Xe MRI showed alveolar-capillary diffusion limitation in all 9 post COVID-19 pneumonia patients despite normal or nearly normal CT scans.

Introduction

There is emerging evidence of long-term challenges for patients after COVID-19 infection, often called 'Long-COVID', with many reporting ongoing symptoms many weeks and months after the acute illness (1). Studies have also shown that patients with SARS-CoV-2 virus may have multi-organ damage that can persist months after discharge (2,3). Two of the commonest symptoms in patients with Long-COVID are fatigue and breathlessness, commonly with no identifiable cause on imaging, lung function or blood tests (4).

Dissolved phase hyperpolarized ^{129}Xe MRI (Xe MRI) enables sensitive, regional investigation of pulmonary ventilation, microstructure and gas transfer across the alveolar epithelium into the blood stream (5–8). The solubility of xenon in the blood in the pulmonary vasculature presents a sensitive method of quantifying ventilation and/or perfusion defects in the lungs (9) and has the advantage of identifying areas of gas exchange mismatch that is not possible by composite measures of global lung function such as that provided by carbon monoxide diffusing capacity (DL_{CO}) measurements (10). An initial study has demonstrated abnormal gas transfer in acutely unwell patients with COVID-19 infection (11). This study aimed to determine if dissolved phase Xe MRI could identify the possible cause of breathlessness in participants more than three months after hospital discharge following COVID-19 infection.

Materials and Methods

The study was approved by our local ethical board (20/NW/0235) and participants were enrolled between August and December 2020. All participants signed an informed consent form and agreed to participate in this study.

Patients were recruited from local respiratory medicine clinics, with the following criteria: positive polymerase chain reaction (PCR) result for SARS-CoV-2, have been hospitalised for COVID-19, and discharged from hospital for at least 3 months. Patients were excluded who had been invasively ventilated during their stay in hospital. Volunteers were recruited from asymptomatic local staff with a negative PCR result for SARS-CoV-2 and no history of cardiac or respiratory disease and imaged to enable reproducibility and comparison with prior Xe MRI publications in patients with interstitial lung disease to be performed. No participant was reimbursed for taking part in this study.

All patients had unenhanced low dose inspiratory volumetric CT performed both at 1 litre inspiration, and then at full expiration, hyperpolarized Xenon MRI, spirometry, and standard biochemistry and haematology tests on the same day, Medical Research Council (MRC) breathlessness and Modified Borg (mBORG) dyspnea scores were collected, and their in-patient imaging was also reviewed. All volunteers had a hyperpolarized Xenon MRI. (See Figure 1 for patient enrollment and investigations.)

Xenon hyperpolarization

^{129}Xe gas (86% 129Xe, Spectra Gases Inc.) was polarized as previously described (12).

Briefly, ^{129}Xe gas (86% 129Xe, Spectra Gases Inc., Ely, Cambs) was polarized by rubidium vapour spin exchange optical pumping (SEOP), and cryogenically accumulated in 1-L doses using a commercial polarizer (Model 9810, Polarean, Durham, NC).

Polarization was measured using a commercial polarisation measurement station (Model 2881, Polarean). Hyperpolarized ^{129}Xe was thawed into a Tedlar® bag (Jensen Inert Products, Coral Springs, FL) and given within 10 minutes of production to participants who were lying supine in the MRI scanner (12).

Hyperpolarized Xenon MRI

XeMRI was performed on a 1.5T GE system (HDx, GE Healthcare, Chicago, IL) with imaging performed on a dedicated ^{129}Xe thorax transmit receive quadrature coil (CMRS, Brookfield, WI) and the ^{1}H body coil (GE Healthcare, Chicago, IL).

A single exponential fit to the integrated gas spectrum was used to calibrate transmit power (assuming ^{129}Xe T_1 of 23s) and centre frequency. A further sodium calibration was performed to estimate gas and dissolved phase centre frequency per participant using pulse acquire non-localised spectroscopic acquisition (hard pulse, pulse width = 500ms, TR = 100ms, flip angle = 20 degrees, number of averages (NEX) = 16) (13).

Dissolved phase ^{129}Xe Images were acquired using a 3D 4-echo flyback radial acquisition as previously described (14) with acquired image resolution of 1.75cm in all dimensions, reconstructed resolution of 0.875cm in all dimensions, repetition time per spoke = 23ms, flip angle per excitation on dissolved and gas phases = 40 and 0.7 degrees, respectively, total scan time = 16s.

Gas, Tissue/Plasma (TP), and Red Blood Cell (RBC) images were reconstructed via matrix inversion of the preconditioned chemical shift encoding matrix in k-space, gridding and Fourier transform (15). The FWHM of the gas, TP, and RBC resonances, from the summed spectra from the calibration acquisition, was calculated after fitting a Lorentzian function in the frequency domain.

The noise level for each image was calculated on a slice-by-slice basis. Any voxels in the TP mask in a given slice that were less than 5 times the median noise level in the slice were discarded. Ratiometric maps (RBC:TP) were then calculated on a voxel-by-voxel basis.

The mean of each ratiometric map was then calculated on a patient-by-patient basis.

CT

CT scanning was performed using a Revolution CT (GE Healthcare, Chicago, IL). Low dose CT scans were performed following inspiration of room air, with a slice thickness of 0.625mm. The CT scans were reviewed by a single reader blinded to the clinical data and hyperpolarized xenon imaging results, on a PACS workstation, for the presence of ground glass opacification, reticulation, traction bronchial dilatation, and honeycombing using a previously published methodology (FG, 30 years of thoracic radiology experience) (16).

Chest X-Ray (CXR)

CXRs were reviewed by a single reader blinded to the blinded to the clinical data, and XeMRI results, using a previously published CXR severity score (FG, 30 years of thoracic radiology experience) (17). For the purpose of the study, the most severe CXR severity score assigned by the reader during the course of the hospitalization was used. Each CXR was divided into 3 zones, and each zone given a binary score dependent upon whether an abnormality was present (score of 1) or absent (score of 0).

Statistical analysis

The coefficient of variation of patient RBC:TP histogram data was calculated. RBC:TP reproducibility was assessed using the intraclass correlation coefficient (ICC). Spearman's correlation was performed between RBC:TP and DLco/spirometry/Hb/D-Dimer results. A Wilcoxon rank-sum test was used to compare mean RBC:TP between patients and controls, and Hodge's effect size was also calculated. Data is shown as mean ± sd. A p-value of 0.05 was considered significant. All analysis was performed in R (r-project.org, v4.0.3).

Results

A flow chart of the study recruitment process is shown in Figure 1. 9 patients (57 ± 7 years, Male = 6) and 5 healthy volunteers (29 ± 3 years, Female = 5) were recruited. Mean time from hospital discharge was 169, range 116-254 days. Patient demographics and clinical details are found in Table 1 and LFTs in Table 2.

Image analysis

Xenon calibration and imaging was successful in all patients, ^{23}Na calibration showed a mean ratio metric difference between ^{23}Na and ^{129}Xe Gas resonances of 0.9563077 ± 0.0000008 and a frequency difference of 771758 ± 14 Hz.

Participant xenon dissolved phase imaging revealed impairment in the transport of gas from the tissue/parenchyma to the red blood cells. There was a difference in RBC:TP between patients and controls (0.3 ± 0.1 versus 0.5 ± 0.1, respectively, p = 0.001, effect size = 1.36). There was a significant difference in the FWHM between controls and patients in the RBC and gas phases (median ± 95 % confidence interval, 567 ± 1 vs 507 ± 81 Hz, p = 0.002 and 104 ± 2 vs 122 ± 17 Hz, p = 0.004, respectively) but not in the TP compartment (420 +- 2 vs 418 +- 57 Hz, p=0.72). See table 3 for numerical results. Participant and volunteers exhibited good subjective image ventilation of the lungs with ^{129}Xe gas on reviewing the images. The mean score of the most severely abnormal in-patient CXRs was 3/6, range 0-6/6. The ICCs for participants and volunteers were 0.82 and 0.88, respectively.

Participants had normal or near normal CT scans, mean 7/25, range 0-10/25. The CT of an example patient taken at the time of their XeMRI can be seen in Figure 2 A-C, with comparative healthy control imaging in D-E. Montages of all patients and volunteers scanned in this study are shown in Figures 3 and 4.

There were no significant correlations between the patient RBC:TP imaging and carbon monoxide diffusing capacity (DL_{CO}, r = -0.08, p = 0.86), age (r = -0.2, p=0.6), D-Dimer (r = -0.55, p = 0.12), Hb (r = 0.17, p = 0.65), forced expiratory volume (r = -0.11, p =0.78), and forced vital capacity (r = 0.53, p = 0.17). There was a strong correlation between Gas and RBC phase FWHM and DLco (R^2 = 0.99 and 0.94, respectively p = 0.04 for both correlations) but not with TP (R^2 = 0.47, p = 0.2).

Discussion

Although the acute illness secondary to SARS-CoV-2 viral infection has been the main focus of research and clinical management, there are increasing reports of persistent symptoms, now called 'Long-COVID', lasting for months after discharge (1), with no apparent reliable clinical or imaging biomarkers (4). Our study has investigated the possible etiology of these symptoms.

The SARS-CoV-2 virus binds to ACE2 receptors for internalization and propagation (18). These receptors are expressed in several groups of cells but type II alveolar epithelial cells are its main site in the lung (18). Upon internalization, the virus repurposes the cells' DNA to create its progeny, killing the host cells and infecting the neighboring cells, causing an increasing amount of alveolar damage (19). Type II alveolar epithelial cells are now known to be the progenitors to the type I alveolar epithelial cells which allows efficient gas exchange (20). Preferential destruction of type II cells following viral infection could impair alveolar repair, reducing the proportion of functioning gas exchange units within lungs. Additionally, COVID-19 disease shows specific immunological abnormalities which could contribute to vascular inflammation, thromboses and long term consequence in alveolar regeneration (21), with persistent functional abnormalities in monocytes promoting low

grade vascular inflammation and hampering repair of the alveolar-epithelial-capillary layer (22), potentially impairing resolution of thrombi in the lungs. These abnormalities are especially relevant to the alveolar unit as the alveolar epithelium and the vessels are in close contact (sharing a basement membrane) (22). Alveolar capillary microthrombi may also contribute to local oxygen starvation of alveolar epithelium after COVID-19 and potentially delaying regeneration of these cells. See Figure 5 for a possible schematic representation of these processes.

Our results are in keeping with the pathogenesis of disease secondary to SARS-CoV-2 virus infection. We have demonstrated lung function impairment using dissolved phase XeMRI in patients, as hallmarked by a significant decrease in RBC:TP between patients and volunteers (0.3 ± 0.1 versus 0.5 ± 0.1, respectively, $p = 0.001$, effect size = 1.36) after COVID-19 infection that is not readily detectable by conventional CT imaging (mean 7/25, range 0-10/25) or lung function tests including DL_{CO}. The abnormalities we have observed specifically reflect the diffusion of xenon across the alveolar epithelium, and therefore the integrity of the alveolar epithelial-capillary structure. This alveolar epithelial damage is presumed to occur at the time of the initial infection, but its persistence and the possible alveolar capillary thrombosis, reported from postmortem studies of patients dying from COVID-19 pneumonia (23) may be contributing to the persistence of symptoms. This hypothesis is supported by our detection of damage more than 3 months post hospital discharge, with one of our patients demonstrating significant pulmonary damage more than 8 months post discharge. Alveolar capillary thrombosis may be one of the contributing factors to Long COVID, but this hypothesis will require substantiation in a larger population of patients post COVID-19 pneumonia, and also in a non-hospitalized cohort of patients with Long COVID. Additionally, we have failed to identify a correlation between XeMRI gas

exchange severity and the D-Dimer measured at the time of scanning ($r = -0.55$, $p = 0.12$), suggesting that the thrombosis happened at the time of the acute infection, and that D-Dimer measurement may not be a reliable indicator of ongoing problems post the acute infection.

The prevalence, duration and resolution or otherwise of these abnormalities is unknown, and these will be critical to determine the health economic burden and management of patients post infection. It is also not known whether patients post other viral pneumonias such as influenza would cause similar abnormalities on XeMRI, although the specific profile of the SARS-CoV-2 virus in comparison to other viruses causing respiratory infection suggests that this is unlikely.

The XeMRI technique we have used has been previously reported (14), and demonstrates good reproducibility for patients and volunteers (0.82 and 0.88, respectively) (24). Using the healthy volunteers as a comparator group, our results to are similar to the published literature (14). The low RBC:TP we are reporting is similar to reports in patients with interstitial lung disease such as idiopathic pulmonary fibrosis but these patients have significantly abnormal CT scans (14), whereas here we demonstrate damage effectively only seen using XeMRI in patients with normal or near normal CT scans. On subjective assessment, our patients demonstrated normal ventilation on XeMRI confirming that the main abnormality and damage caused by the SARS-CoV-2 virus is in areas of pulmonary gas exchange and is present diffusely throughout the lungs as shown by the wide coefficient of variation.

The DL_{CO} results did not correlate with the RBC:TP imaging results ($r = -0.08$, $p = 0.86$) and were within the normal ranges for our patients. This suggests that XeMRI is potentially a more sensitive technique in detecting pulmonary damage from COVID-19

pneumonia than lung function tests including DL_{CO} and may be better placed to explain breathlessness in patients with Long COVID, specifically in those with normal or near normal CT scans.

Our study is limited by the small sample size for both patient and volunteer groups, however it is worth noting that our findings were consistent across all patients. It is also important to note that the patients included did not have severe COVID-19 pneumonia requiring ventilation or prolonged ITU stays, and only two had pulmonary emboli identified when an in-patient, suggesting that the damage detected is due to the virus and not secondary to superadded infection, trauma from ventilation, or pulmonary embolic disease. Another limitation of the study here is the small, non-age matched control group, however in a larger study in healthy controls, age range 30-65 years, median age 38 years (14) using the exact same pulse sequence and model of RF coil and MRI scanner, a mean RBC:TP of 0.47 was found, which is consistent with this study. Age causes only a modest reduction in DLco rather than the larger reduction in the RBC:TP that we are reporting here post COVID (25,26). Although smoking is known to reduce DLco (27), it is of note that one of the two participants with a smoking history in this study had a higher DLco than some of the non-smoking participants. It will be important for future work to compare patients with different disease status post COVID infection such as those that have fully recovered, those post-ITU discharge, those with proven embolic disease, and an age matched healthy control group with a larger cohort of the population we have studied. It will also be important to identify whether the abnormalities detected correlate with clinical symptoms.

Although our small study did not recruit from long-COVID clinics, the results suggest that hyperpolarized Xenon MRI may be a potentially useful imaging modality in dyspneic patients with Long-COVID, following hospital discharge at a mean of 3 months for COVID-19.

XeMRI appears to provide an explanation for patient symptoms not explained by other clinical data or imaging techniques, does not pose a radiation burden to the patient and can be completed in a single breath hold. XeMRI may also provide information on the extent to which gas exchange units in the lungs are affected, their duration and the time it takes for regeneration and recovery to occur.

References

1. Halpin SJ, McIvor C, Whyatt G, et al. Postdischarge symptoms and rehabilitation needs in survivors of COVID-19 infection: A cross-sectional evaluation. J Med Virol. 2020; doi: 10.1002/jmv.26368.

2. Carfi A, Bernabei R, Landi F. Persistent Symptoms in PatientsAfterAcuteCOVID-19. JAMA. 2020;324(6):603–605. doi: 10.1056/NEJMp2014836.

3. Puntmann VO, Carerj ML, Wieters I, et al. Outcomes of Cardiovascular Magnetic Resonance Imaging in Patients Recently Recovered from Coronavirus Disease 2019 (COVID-19). JAMA Cardiol. 2020;2019:1–9. doi: 10.1001/jamacardio.2020.3557.

4. Garrigues E, Janvier P, Kherabi Y, et al. Post-discharge persistent symptoms and health-related quality of life after hospitalization for COVID-19. J Infect. 2020;13(21):1–3. doi: 10.1016/j.jinf.2020.08.029.

5. Kaushik SS, Robertson SH, Freeman MS, et al. Single-breath clinical imaging of hyperpolarized 129xe in the airspaces, barrier, and red blood cells using an interleaved 3D radial 1-point Dixon acquisition. Magn Reson Med. 2016;75(4):1434–1443. doi: 10.1002/mrm.25675.

6. Qing K, Ruppert K, Jiang Y, et al. Regional mapping of gas uptake by blood and tissue in the human lung using hyperpolarized xenon-129. J Magn Reson Imaging. 2014;39(2):346–359. doi: 10.1002/jmri.24181.Regional.

7. Weatherley ND, Stewart NJ, Chan HF, et al. Hyperpolarised xenon magnetic resonance spectroscopy for the longitudinal assessment of changes in gas diffusion in IPF. Thorax. 2019;74(5):500–502. doi: 10.1136/thoraxjnl-2018-211851.

8. Hatabu H, Ohno YMP, Gefter WB,. M, et al. Expanding applications of pulmonary MRI in the clinical evaluation of lung disorders: Fleischner society position paper. Radiology. 2020;297(2):286–301. doi: 10.1148/RADIOL.2020201138.

9. Mugler JP, Altes TA. Hyperpolarized 129Xe MRI of the human lung. J Magn Reson Imaging. 2013;37(2):313–331. doi: 10.1002/jmri.23844.

10. Graham BL, Brusasco V, Burgos F, et al. 2017 ERS/ATS standards for single-breath carbon monoxide uptake in the lung. Eur Respir J. 2017;49(1):1–31. doi: 10.1183/13993003.00016-2016.

11. Li H, Adv S, Li H, et al. Damaged lung gas-exchange function of discharged COVID-19 patients detected by hyperpolarized 129 Xe MRI. Sci Adv. 2020;8180(November):1–14. doi: 10.1126/sciadv.abc8180.

12. Chen M, Doganay O, Matin T, et al. Delayed ventilation assessment using fast dynamic hyperpolarised Xenon-129 magnetic resonance imaging. Eur Radiol. European Radiology; 2020;30(2):1145–1155. doi: 10.1007/s00330-019-06415-1.

13. Grist JT, Sánchez-heredia ESSHJD, Mclean MA, et al. Creating a clinical platform for carbon-13 studies using the sodium-23 and proton resonances. Magn Reson Med. 2020;00(1):1–11. doi: 10.1002/mrm.28238.

14. Collier GJ, Eaden JA, Hughes PJC, et al. Dissolved 129Xe lung MRI with four-echo 3D radial spectroscopic imaging: Quantification of regional gas transfer in idiopathic pulmonary fibrosis. Magn Reson Med. 2020;(October):1–12. doi: 10.1002/mrm.28609.

15. Wiesinger F, Weidl E, Menzel MI, et al. IDEAL spiral CSI for dynamic metabolic MR imaging of hyperpolarized [1-13C]pyruvate. Magn Reson Med. 2012;68(1):8–16. doi: 10.1002/mrm.23212.

16. Han X, Fan Y, Alwalid O, et al. Six-Month Follow-up Chest CT findings after Severe COVID-19 Pneumonia. Radiology. 2021;1(1):203153. doi: 10.1148/radiol.2021203153.

17. Toussie D, Voutsinas N, Finkelstein M, et al. Clinical and chest radiography features determine patient outcomes in young and middle-aged adults with COVID-19. Radiology. 2020;297(1):E197–E206. doi: 10.1148/radiol.2020201754.

18. Chung MK, Karnik S, Saef J, et al. SARS-CoV-2 and ACE2: The biology and clinical data settling the ARB and ACEI controversy. EBioMedicine. Elsevier B.V.; 2020;58. doi: 10.1016/j.ebiom.2020.102907.

19. Mason RJ. Pathogenesis of COVID-19 from a cell biology perspective. Eur Respir J. 2020;55(4):9–11. doi: 10.1183/13993003.00607-2020.

20. Rawlins EL, Hogan BLM. Epithelial stem cells of the lung: Privileged few or opportunities for many? Development. 2006;133(13):2455–2465. doi: 10.1242/dev.02407.

21. Varga Z, Flammer AJ, Steiger P, et al. Endothelial cell infection and endotheliitis in COVID-19. Lancet. 2020;395(May):1417–1418.

22. Vlacil AK, Schuett J, Schieffer B, Grote K. Variety matters: Diverse functions of monocyte subtypes in vascular inflammation and atherogenesis. Vascul Pharmacol. 2019;113(December 2018):9–19. doi: 10.1016/j.vph.2018.12.002.

23. Ackermann M, Verleden SE, Kuehnel M, et al. Pulmonary Vascular Endothelialitis, Thrombosis, and Angiogenesis in Covid-19. N Engl J Med. 2020;383(2):120–128. doi: 10.1056/nejmoa2015432.

24. Koo TK, Li MY. A Guideline of Selecting and Reporting Intraclass Correlation Coefficients for Reliability Research. J Chiropr Med. Elsevier B.V.; 2016;15(2):155–163. doi: 10.1016/j.jcm.2016.02.012.

25. Crapo RO, Morris AH. Standardized single breath normal values for carbon monoxide diffusing capacity. Am Rev Respir Dis. 1981;123(2):185–189. doi: 10.1164/arrd.1981.123.2.185.

26. Olfert IM, Balouch J, Kleinsasser A, et al. Does gender affect human pulmonary gas exchange during exercise? J Physiol. 2004;557(2):529–541. doi: 10.1113/jphysiol.2003.056887.

27. Sherrill DL, Enright PL, Kaltenborn WT, Lebowitz MD. Predictors of longitudinal change in diffusing capacity over 8 years. Am J Respir Crit Care Med. 1999;160(6):1883–1887. doi: 10.1164/ajrccm.160.6.9812072.

Table 1: Participant Clinical Details

No	Gender	Age (years)	Hospital length (days)	Supplemental oxygen	Pulmonary Embolus	Time from discharge to imaging (days)	Smoking history	D-Dimer Normal range (0-250 ng/mL)	Hb	DLCO (%) Normal range 80-120%	MRC breathlessness (0-1)	mBORG dyspnea score (0-1)	Pulse oximetry (% at scan)	Outpatient CT score (Potential range 0-25)
1	M	62	4	yes 4L	No	129	Never	197	156	90.9	2	1	>96	10
2	M	60	5	yes 2L	No	169	Unknown	279	142	117.3	0.5	1	>96	4
3	M	68	3	yes 4L	No	116	Never	395	160	83.7	1	0.5	>96	0
4	F	51	8	yes 1L	Yes	254	Never	260	116	99.7	2	1	>96	0
5	F	56	3	No	No	134	Never	213	122	92.2	2	3	>96	2
6	M	56	3	No	Yes	191	Never	195	134	89.1	2	1	>96	7
7	M	65	9	yes *NHFO/CPAP	No	150	10 pack/year	1982	146	95	2	3	>96	9
8	M	55	6	Yes 2L	No	110	Never	189	133	N/A	2	1	>96	9
9	M	65	3	No	No	212	8 pack/year	329	146	N/A	1	0.5	>96	0

NHFO/CPAP = Nasal High Flow Oxygen/Continuous Positive Airway Pressure, D-Dimer = Domain Dimer , DLco = Diffusing capacity of the lungs for Carbon Monoxide, MRC = Medical Research Council, mBORG = Modified Borg, CT = Computed Tomography, N/A = Not available.

Table 2: Pulmonary Function Test Results of the Participants 3 Months or More after Recovery from Hospitalization from COVID-19 Pneumonia

	Age	Sex	FEV1 (%)	FVC (%)	FEV1/FVC	DL_{CO} (%)
1	62	M	94.7	91.1	1.04	90.9
2	60	M	112	113.9	0.98	117.3
3	68	M	73.9	114.7	0.64	83.7
4	51	F	106.5	96.8	1.10	99.7
5	56	F	109	107	1.02	92.2
6	56	M	101	137	0.74	89.1
7	65	M	109	110	0.99	95
8	55	M	N/A	N/A	N/A	N/A
9	65	M	N/A	N/A	N/A	N/A

FEV1 = Forced Expiratory Volume after 1 second, FVC = Forced Vital Capacity, N/A = Not available.

Table 3: Comparison of the Median Values for the XeMRI Global Spectral Full Width Half Maximum Peaks for Ventilation, Barrier and RBC for the Nine Participants 3 More Months after Recovery from COVID Pneumonia and the Five Normal Volunteers

XeMRI FWHM	Normal volunteers (HZ, median +- 95% Confidence interval)	Participants (Hz, median +- 95% Confidence interval)	P value
Median RBC peak	567 +- 1	507 +- 81	p = 0.001
Median Barrier	420 +- 2	418 +- 57	p = 0.72
Median Ventilation	104 +- 2	122 +- 17	p = 0.004

FWHM = Full Width at Half Maximum, RBC = Red Blood Cell.

Figures

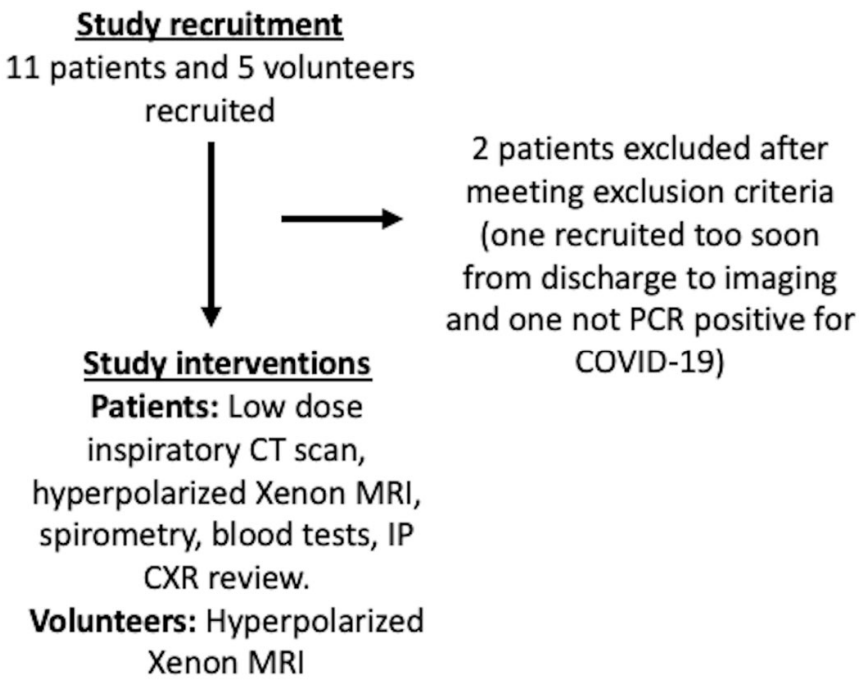

Figure 1: Study flowchart.

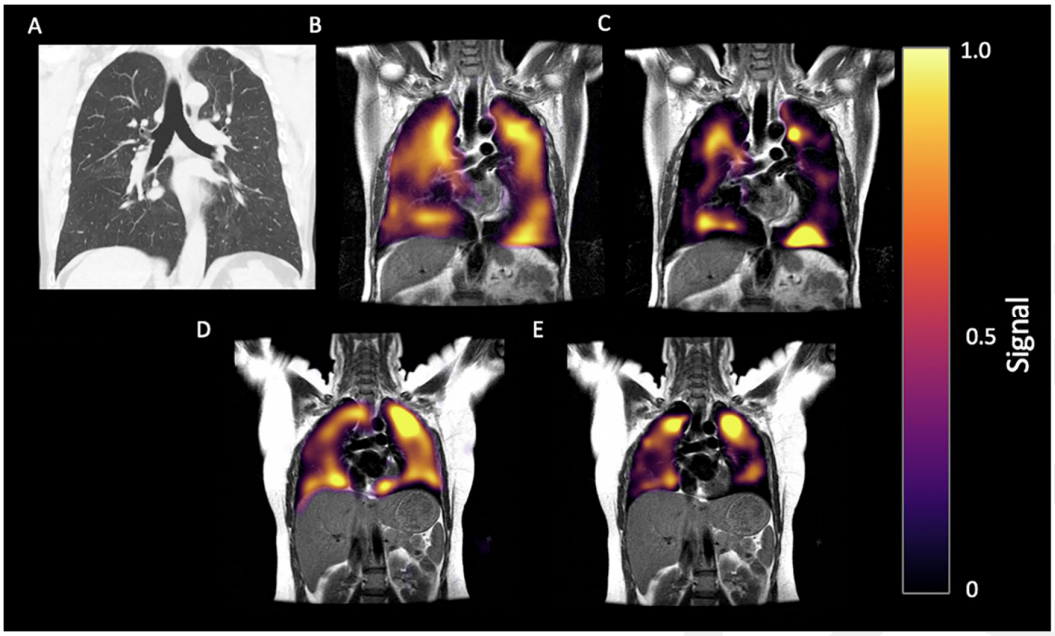

Figure 2: 60-year-old man with history of post-COVID breathlessness, shown 172 days after discharge. (A) CT, (B) Ventilation and (C) RBC phase imaging. (D) Gas and (E) RBC phase imaging for a healthy control. ^{129}Xe MRI images shown in the coronal view for both, with disrupted RBC in the patient.

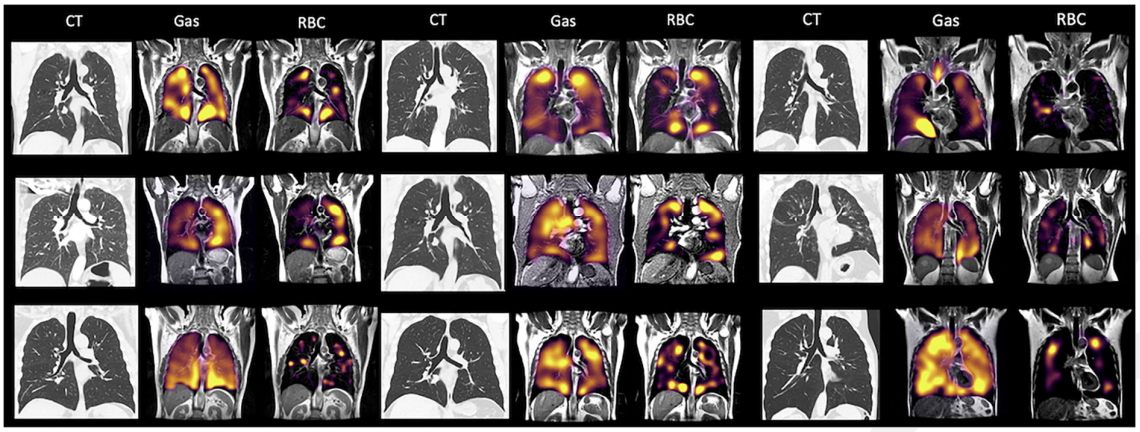

Figure 3: A montage of all patients scanned in this study showing CT, Gas, and RBC phase imaging in the coronal plane.

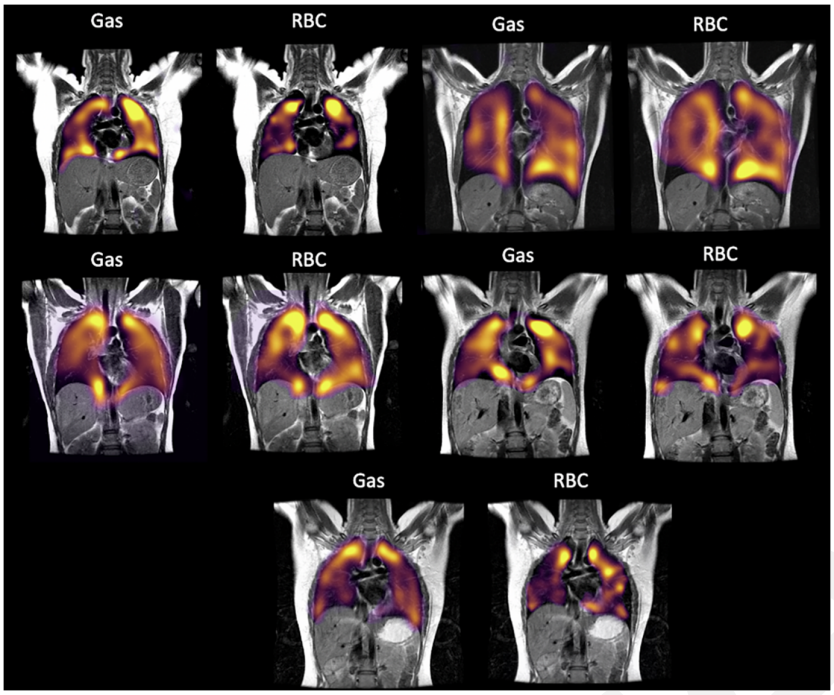

Figure 4: A montage of all volunteers scanned in this study showing Gas and RBC phase imaging.

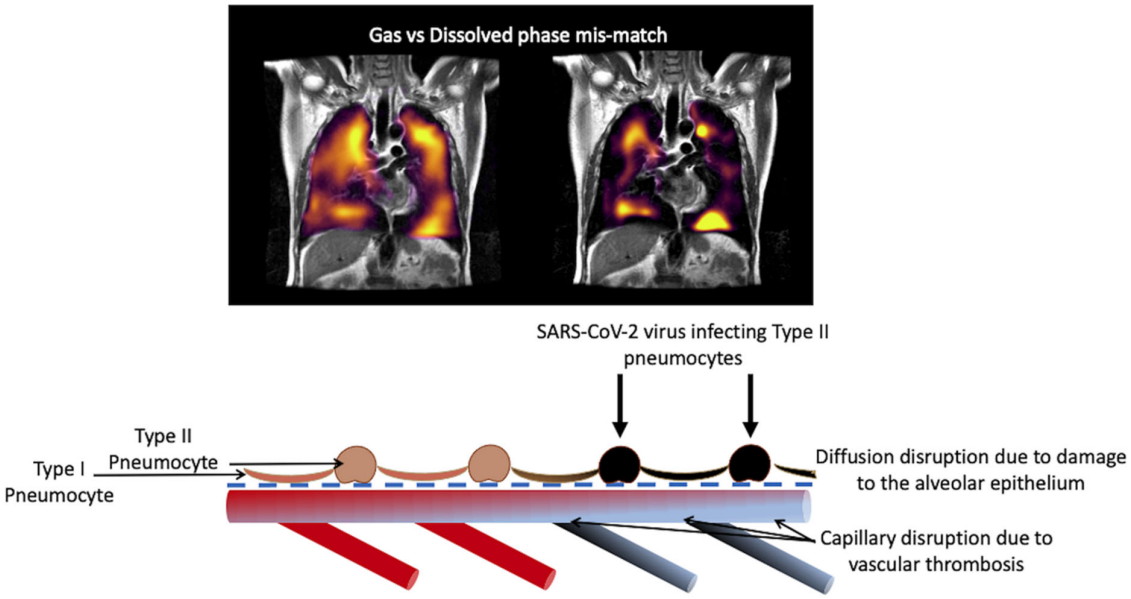

Figure 5: Schematic drawing of the processes leading to gas-dissolved phase mismatch post-COVID.